Journal of Fundamental and Applied Sciences

ISSN 1112-9867

Available online at http://www.jfas.info

Research Article

Special Issue

DEVELOPMENT OF LOW POWER WIRELESS FLUXGATE MAGNETOMETER INSTRUMENTATION FOR REAL-TIME GEOMAGNETIC MONITORING

A. F. Z. Abidin[1,2,*], M. H. Jusoh[1,2], S. A. M. A. Junid[1] and A. H. A. Razak[1]

[1]Faculty of Electrical Engineering, UniversitiTeknologi MARA, 40450 Shah Alam, Selangor, Malaysia

[2]Applied Electromagnetic Research Center, UniversitiTeknologi MARA, 40450 Shah Alam, Selangor, Malaysia

Published online: 17 October 2017

ABSTRACT

Current magnetometers for continuous geomagnetic monitoring are costly, discrete part by part system and require authority permission due to facility needed to sustain the operation such as on-grid power supply and field permission. In this research project, a low cost and mobile magnetometer was designed to overcome the stated issues. The developed magnetometer consists of only two units system which consists of magnetometer and data acquisition units. These two units communicate via IEEE 802.11 Wireless Local Area Network (WLAN). Horizontal (H) and field intensity (F) components magnetic parameters shows reading uniformity with the existing observatory, while declination (D) and vertical (Z) component graph pattern strongly effected by local activities, the details of the magnetometer development will be discussed in the paper.

Keywords: wireless magnetometer; geomagnetic; fluxgate; wireless data acquisition.

Author Correspondence, e-mail: ahmadfaizal91@gmail.com

doi: http://dx.doi.org/10.4314/jfas.v9i5s.34

Journal of Fundamental and Applied Sciences is licensed under a Creative Commons Attribution-NonCommercial 4.0

1. INTRODUCTION

Magnetic field is one of the fundamental physical parameters of solar terrestrial physics field in order to study the origin and evolution of universe [1]. Magnetometer is a scientific instrumentation to measure magnetic field variation over time used to observe the magnetic field interaction of solar activity and near-Earth magnetic field. Magnetometer also plays an important role in various applications field such as security, medical, electronics mechanism, material science and geophysics [2].

The study of space weather physics is the study of the active interactions between solar wind magnetize plasma and magnetosphere that is observed by arrays of magnetometer installed around the Earth [3-4]. The Earth's magnetic field magnitude is in the range of 20,000nT to 65,000nT depends on location point based on magnetic field contour line as can be seen in isodynamic chart from world magnetic model [5]. Exogenous effect on Earth's magnetic field can cause numerous consequences on natural and human made technology [6-7]. Satellite operation is strongly dictated by near-Earth orbit space weather condition [8]. At Earth's high latitude region, geomagnetic storm can cause the phenomena called "the northern lights" or aurora borealis [9]. The modern space physics human knowledge is intimately linked to development of magnetic field instrumentation and its ability [10].

In this research, the technology used in the geomagnetism magnetometer is re-examined and up-to-date commercially available technology is implemented. Commercially available technology significantly reduce the manufacturing cost and project time. By reducing the manufacturing cost, the instrumentation availability could be increased and perhaps solving the stated issues. As huge benefit lies behind the technology, currently it is being targeted as a science education teaching tools especially in first country [10].

Fluxgate type magnetometer sensor has good practicality for geomagnetic field vector measurement as fluxgate magnetometer sensor has decent trade-off between performance, noise, stability, cost and physical dimensions made it still relevant to be used till nowadays. To replace the cable function, the serial data is sent over IEEE802.11 WLAN to DAQ unit.

2. METHODOLOGY

There are two standard ways two define magnetic field vector representation, first is XYZ and

second is HDZ vector representation. In this paper, the HDZ vector representation is selected. The tri-axial wireless fluxgate magnetometer configuration is set up based on in situ magnetic field vector alignment, which X-axis sensor is pointing towards magnetic north, Y-axis sensor is pointing towards 90˚ clockwise (eastward) relative to X-axis and Z-axis sensor is pointing towards positive vertical direction (where will be corrected to downward vertical magnitude by the data acquisition algorithm).

From the tri-axial setup, the HDZ vector data can be obtained through DAQ algorithm where the horizontal component (H-component) is formulated in Equation (1),

$$H = \sqrt{X^2 + Y^2} \tag{1}$$

D-component or declination component can be obtained based on Equation (2),

$$D = \cos^{-1}\frac{X}{H} \tag{2}$$

And the Z component or vertical component is obtained by inverting the Z-axis sensor data, Z_M to get the downward vertical component as stated in Equation (3),

$$Z = -Z_M \tag{3}$$

The magnitude of the obtained data is compared with isodynamic chart from British Geological Survey (BGS). The 2015 magnetic field contour maps of H-, D- and Z-component respectively can be referred in Fig. 2, Fig. 3 and Fig. 4.

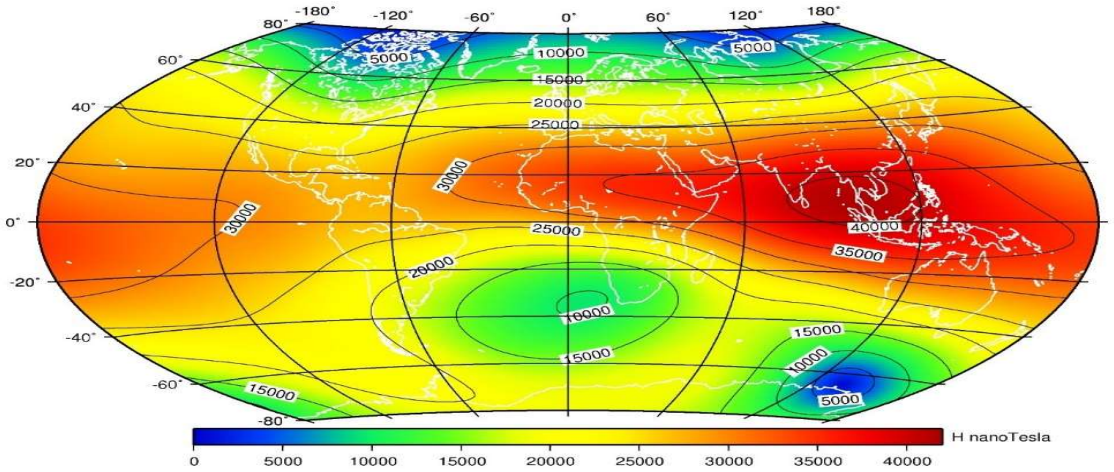

Fig.1.BGS modelling of 2015 H-component contour map

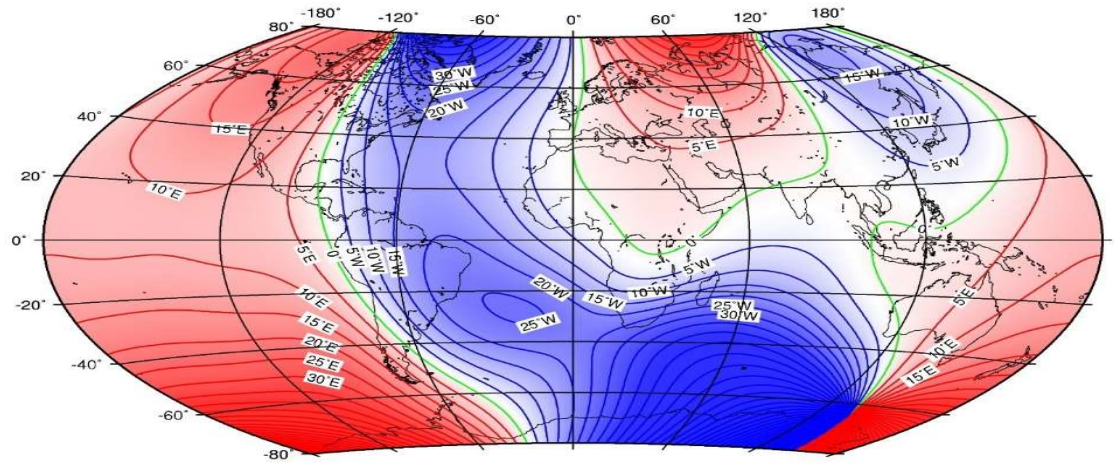

Fig.2.BGS modelling of 2015 D-component contour map

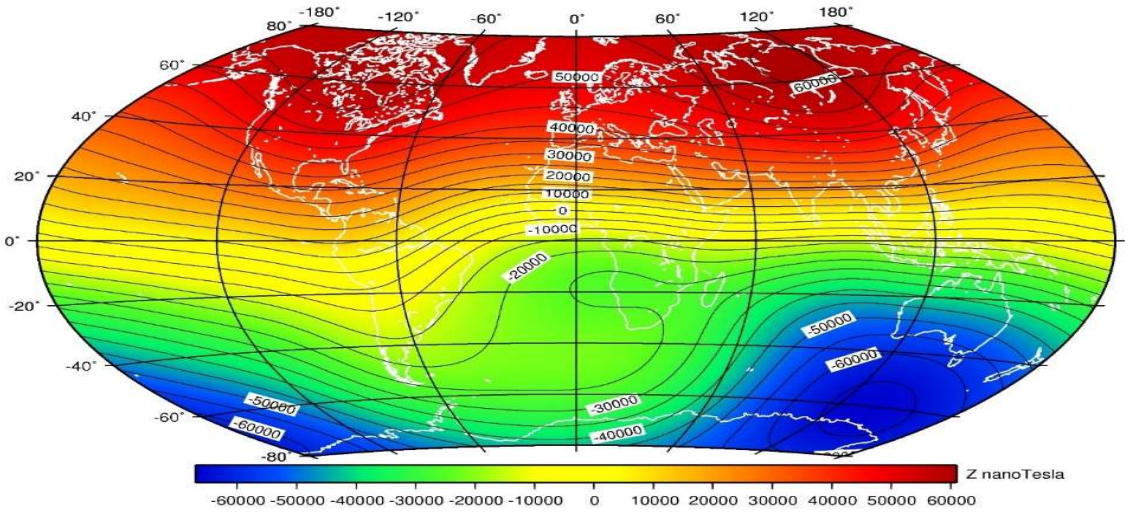

Fig.3.BGS modelling of 2015 Z-component contour map

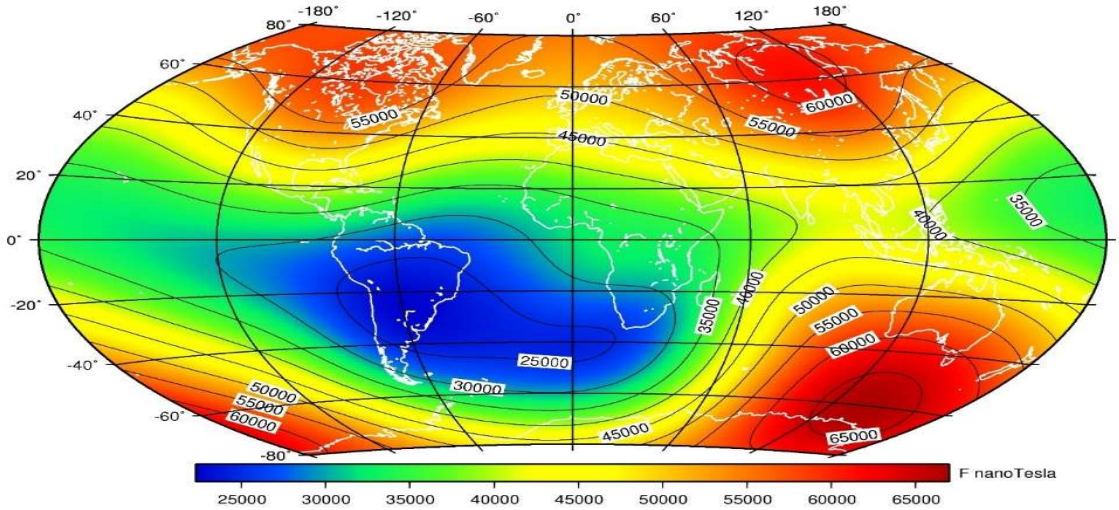

Fig.4.BGS modelling of 2015 F-component isodynamic chart

3. SYSTEM ARCHITECTURE AND DEVICE MECHANISM

The magnetic field reading is interpreted based on changes of frequency readings due to perturbation from external magnetic field towards induction coil inside the digital fluxgate sensor. Based on device architecture and mechanism in Fig. 5, the pulse width modulation (PWM at 0-5V DC) frequency pulse stream readings is fed into microcontroller unit and the frequencies reading are read by frequency counter algorithm by counting the number of rising edge via external interrupt and translated into digital binary readings.

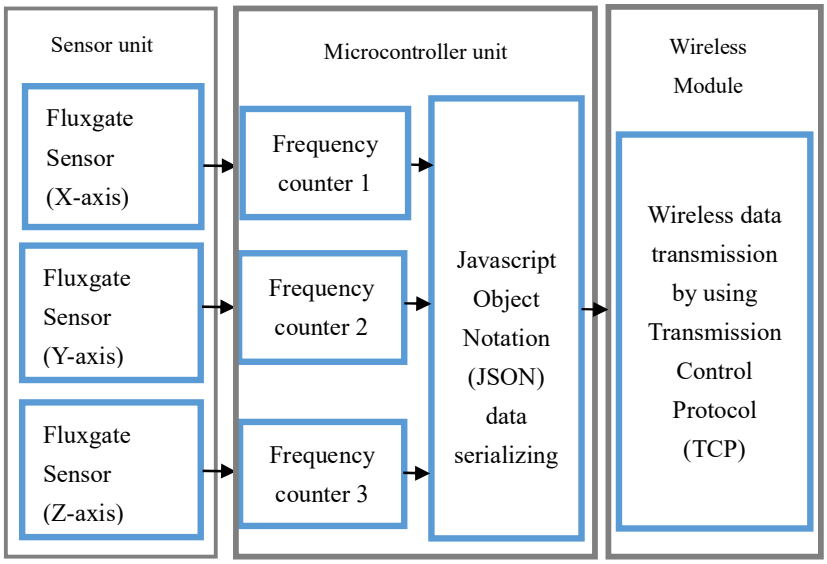

Fig.5. Wireless fluxgate magnetometer device mechanism and architecture

The square wave frequencies pulses from the fluxgate sensors behave as an external clock for microcontroller and the rising edges of the square waves are counted within single gate timing period, which is set in the microcontroller unit to 500 milliseconds and times by two to obtain standard frequency reading with a fast response. The device under testing (DUT) can be seen in Fig. 6.

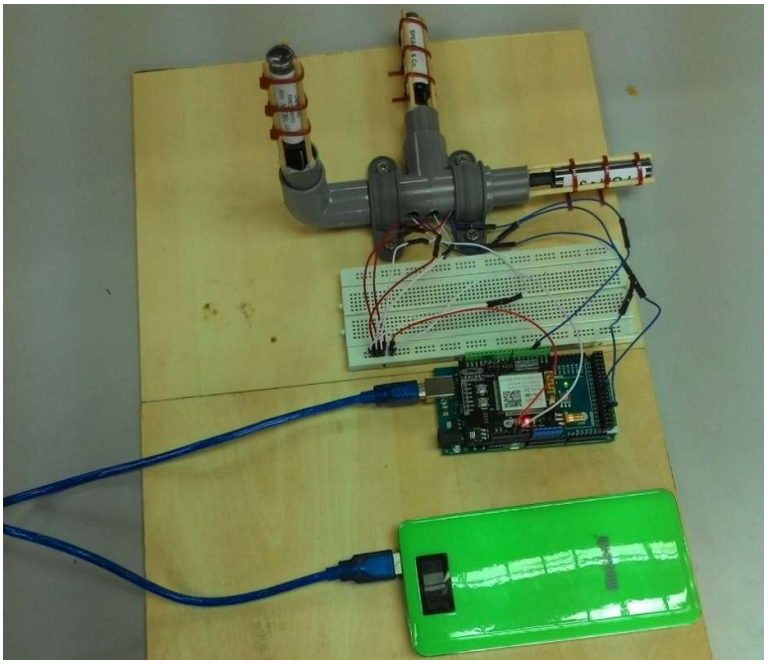

Fig.6. The device under testing (DUT) wireless magnetometer circuit and setup

The tri-axial frequencies reading are serialized by java script object notation (JSON) with 200 bytes buffer since the microcontroller has small Static Random Access Memory (SRAM) to perform software task as the Atmel Atmega2560 microcontroller has only 8kilobytes SRAM with 8-bit Central Processing Unit (CPU). The serialized frequencies data is transferred to wireless module via Universal Asynchronous Receiver/Transmitter (UART) interface and the wireless module transmitting the serialized frequencies data to data acquisition (DAQ) unit through Transmission Control Protocol (TCP) transport layer at 1Hz sampling rate.

At the DAQ unit, the serialized frequencies data are decoded and the data are accessed individually based on axis component. The frequencies data are converted into magnetic field reading based on period-magnetic field reading characteristic graph provided by sensors manufacturer as can be seen in Fig. 7.

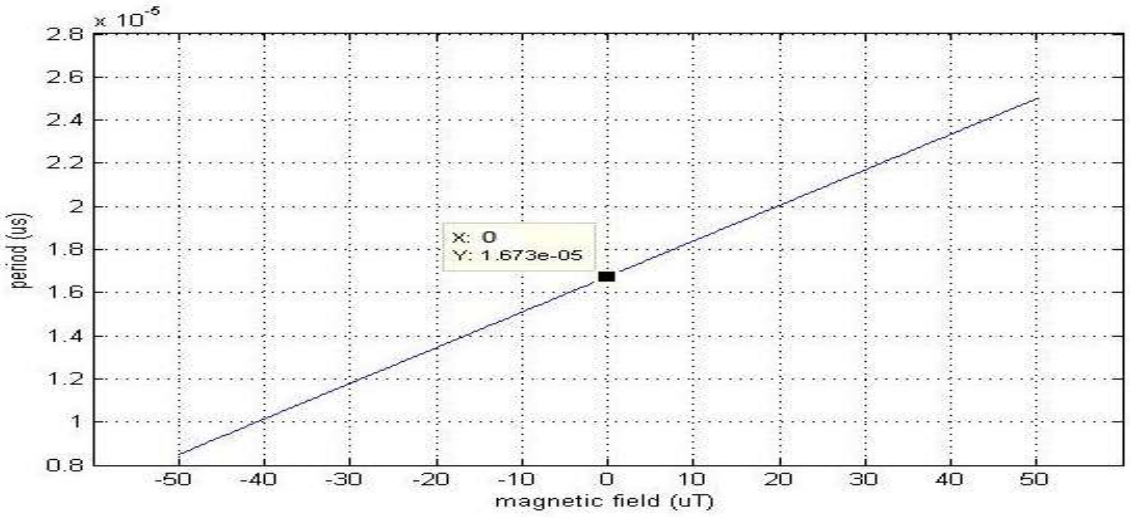

Fig.7. Period-magnetic field characteristic graph provided by the sensor manufacturer

The period to magnetic field reading conversion can be done based on linear Equation (4):

$$y = mx + c \tag{4}$$

where y is equal to period (T), x is magnetic field (B) and c is period value when intercepting at x = 0 which in this case c = 1.673×10^{-5}s. Gradient (m) can be obtained based on the following Equation (5) and (6),

$$m = \frac{\Delta y}{\Delta x} \tag{5}$$

$$m = \frac{y_2 - y_1}{x_2 - x_1} \tag{6}$$

In this case,

$$m = \frac{T_2 - T_1}{B_2 - B_1} \tag{7}$$

$$m = \frac{(1.838 \times 10^{-5}\text{s}) - (2.168 \times 10^{-5}\text{s})}{(10\,000\ \text{nT}) - (30\,000\ \text{nT})} \tag{8}$$

$$m = 1.65 \times 10^{-10}\text{s nT}^{-1} \tag{9}$$

Based on the information obtained from Equation (9), then,

$$T = mB + c \tag{10}$$

$$T = (1.65 \times 10^{-10}\text{s nT}^{-1}) + (1.673 \times 10^{-5}\text{s}) \tag{11}$$

The magnetic field value can be obtained based on the Equation (12) and implemented in the period to magnetic data conversion algorithm in the microcontroller unit,

$$T = \frac{T - (1.673 \times 10^{-5}\text{s})}{1.65 \times 10^{-5}\text{s nT}^{-1}} \tag{12}$$

3.1. Fluxgate Magnetometer Sensors

Fundamental working principle of fluxgate is mutual induction between drive coil and sense coil, then by the superimposed effect of both coils is interpreted as the output reading [11]. The sensor core is excited through drive winding and saturates alternately in either direction. Mutual induced voltage interact with external magnetic field and induces voltage in the pickup coil, based on Faraday's law in Equation (13):

$$V = -N \cdot \frac{d\emptyset}{dt} \tag{13}$$

where V is induced voltage, N is the number of turns and $\frac{d\emptyset}{dt}$ is the rate of change of magnetic flux.

Fluxgate magnetometer sensor is directional magnetic field sensors based on non-linearity of the magnetization of soft-ferromagnetic materials [12]. In this research, the tri-axial fluxgate sensor is put orthogonally to one another forming the three axis sensing in terms of Earth's magnetic field coordinate where X_M is the component pointing to magnetic north, Y_M pointing to magnetic east and Z_M points vertically downward.

The fluxgate sensor is operated with 5.0V±0.5V and 12mA current per axis, which the power consumption per axis is equal to 0.06W. Square wave output pulse is generated from the sensor and the number of pulse generated per second (the frequency) is inversely proportional to the strength of magnetic field. The magnetic field range can be detected linearly up to 50,000nT (with fluxgate frequency output varies in between ~40 kHz to ~120 kHz) and can be increased up to 70,000nT with 15 kHz crystal puller. Come in compact size, with the physical dimensions is equal to 62mm x 16mm. The resolution of these sensors are 10nT, small enough to detect geomagnetism perturbation.

3.2.Microcontroller Unit

Two microcontroller integrated circuit based on Atmel™ AVR platform was chosen. For the main microcontroller unit, it consists of four 16-bit counter which is serving as the external interrupt frequency counter, the tri-axial magnetometer sensors output are directly fed into external interrupt counter pins and calculated based on algorithm calculation and setup. For the second microcontroller, it is used for UART serial communication bridging between computer and main microcontroller. Peripherals are attached to the main microcontroller unit

while the second microcontroller unit is for serial communication task and main microcontroller burner.

The main microcontroller, a low power Atmel™ AVR 8-bit microcontroller series, Atmel™ ATmega2560 model consist of four 16-bit timer/counter with separate prescaler, compare- and capture mode as this is the most useful features in this project. The microcontroller [17] operate with 16MHz clock speed, 256kB in-system programmable flash, 4kB EEPROM and 8kB SRAM. The operating voltage 5.0V±0.5V.

Instead of using microcontroller burner, the USB to serial converter is carried by Atmel ATmega16U2, which makes the serial communication smooth and on-board. The magnetometer is directly powered by 5VDC USB connection instead of using 9V DC jack. The benefit in here, the circuit element could be reduced by the absence of voltage regulator for stepping down the DC voltage into 5V. At the same time, the energy efficiency could be increase as there no electric energy dissipated into heat energy directly as the linear voltage regulator does. The 2-in-1 concept is used in here, which is the USB connection is apply for serial communication at the same time can be used for device power up.

3.3 Data Acquisition (DAQ) Unit

Data acquisition module is a central processing device for data managing and processing. A system-on-chip (SoC) development board is selected to carry the software task, which enough to perform data acquisition [18] application. The SoC development board is consists of Broadcom BCM2835 SoC chip with ARM11 core architecture, which can perform 700MHz computer clock speed, 512MB Synchronous Dynamic Random Access Memory (SDRAM) and detachable micro secure digital (SD) memory card (can be up to 64GB nowadays). With dimensions 85mm x 56mm x 17mm, which about credit card size can compromise the DAQ mobility and physical dimension saving. The DAQ unit receive data feed from sensor unit via IEEE802.11 WLAN and serve as Transmission Control Protocol (TCP) client.

4. RESULTS AND DISCUSSION

A series of experiment of laboratory measurement has been done from 1100UT on 11th March 2015 to 1100UT on 12th March 2015 for 24-hours measurement, which was performed at Microwave Laboratory, Level 7, Faculty of Electrical Engineering, UiTM Shah Alam,

Selangor, Malaysia (coordinate: 3.072˚N, 101.498˚E). From the experiment, the data obtained are plotted based on magnetic field vector components parameter versus concurrent universal time with inclination component, I = 0.29-0.30 (inclination obtained on flat table surface). The recorded geomagnetic field components are compared with the existing Magnetic Data Acquisition System (MAGDAS) established by International Center for Space Weather Science and Education Kyushu University (ICSWSE) and National Space Agency (ANGKASA) at Langkawi (LKW) station during 15th-16th June 2014.

4.1. Data Acquisition and Data Processing

Frequencies data reading from tri-axial magnetometer sensors fed into DAQ unit and directly converted into period reading. To obtain the magnetic field reading, the Equation (8) period-to-magnetic field conversion algorithm is used to convert all tri-axial reading into magnetic field data reading according to sensor axial respectively.

The frequency reading from x-axis sensor varies in the range of 42.250kHz (42,060nT) to 42.370kHz (41,660nT), y-axis sensor varies in the range of 59.180kHz (1009nT) to 59.630kHz (249.7nT) and z-axis sensor varies in the range of 68.200kHz (-12.520nT) to 68.560kHz (-13,000nT) as shown in Fig. 8., Fig. 9 and Fig. 10 respectively align with local geomagnetic field setup.

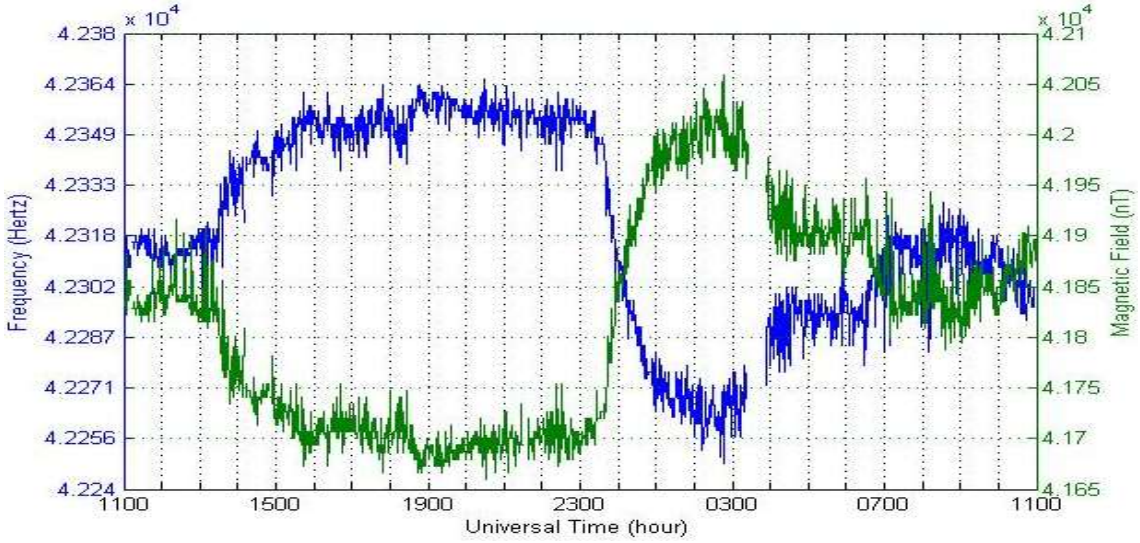

Fig.8. X-axis sensor input frequency reading received from wireless magnetometer (blue line) and output magnetic field data reading (green line)

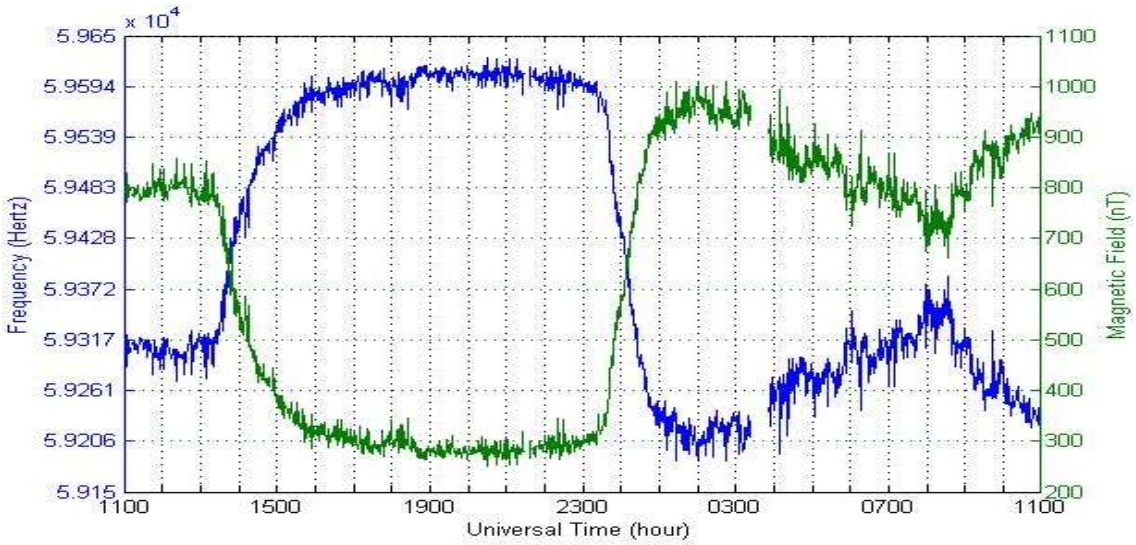

Fig.9. Y-axis sensor input frequency reading received from wireless magnetometer (blue line) and output magnetic field data reading (green line)

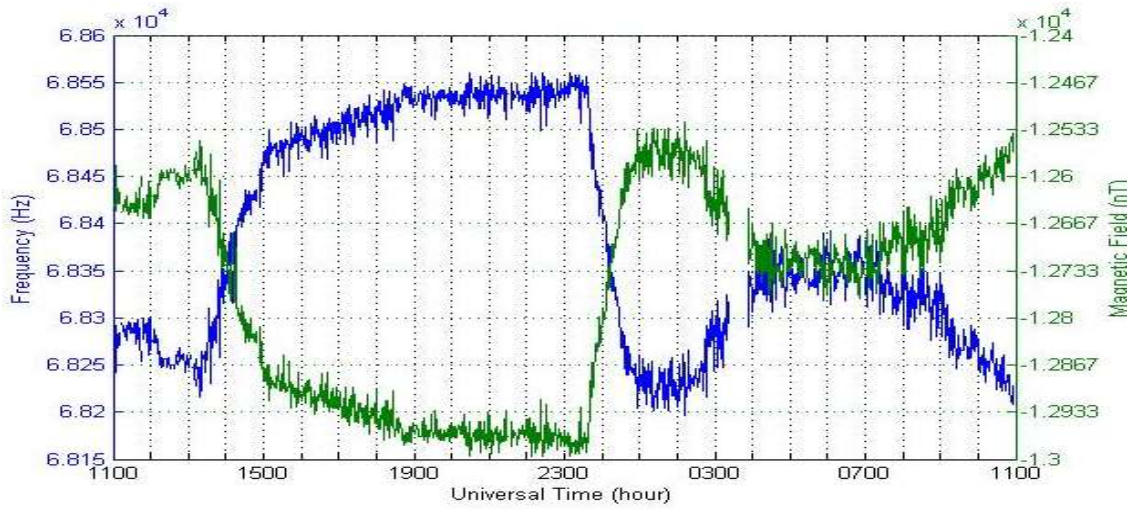

Fig.10. Z-axis sensor input frequency reading received from wireless magnetometer (blue line) and output magnetic field data reading (green line)

The DAQ unit acts as the data processing unit, which carry the function of data conversion, smoothing and further data parameter expansion. From the X-, Y- and Z-axis data reading, further parameter elaboration that extend into H-, D- and Z-component parameter enabled.

4.2. Geomagnetic Field

The D-component data output is plotted in Fig. 11, the data reading shows consistent magnetic field magnitude to isodynamic chart reading where the declination reading at Peninsular Malaysia is varies approximately to 0˚.

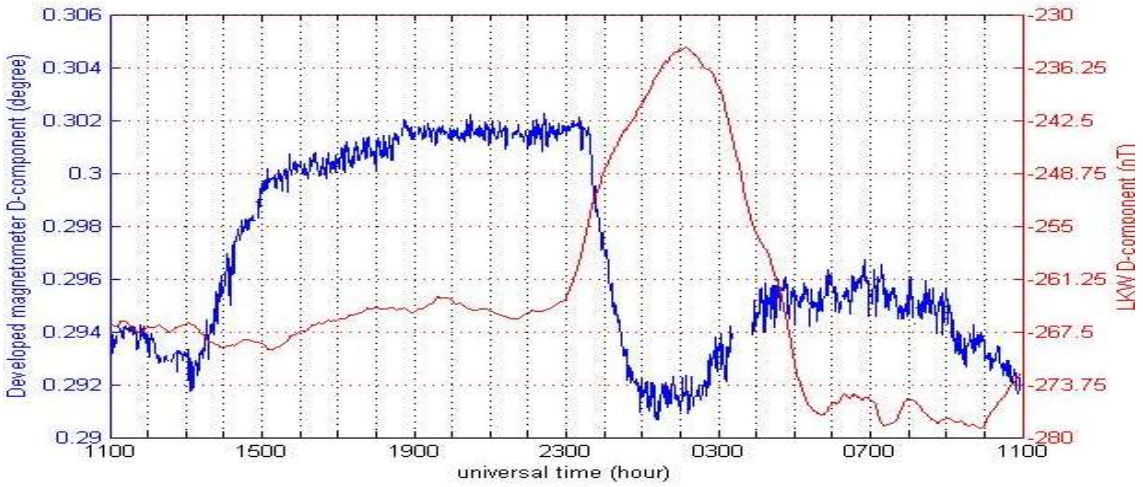

Fig.11. D-component versus universal time from developed wireless fluxgate magnetometer

The developed magnetometer success to show consistent reading output with the H-component isodynamic chart from BGS. The reading magnitude is uniform with the isodynamic chart from BGS for peninsular Malaysia, which based from the contour line is around 40,000nT.

The developed wireless fluxgate magnetometer H-component data is plotted and compared with LNO H-component that is plotted on the same graph figure shown in Fig. 12. During the absent of sunlight, the developed wireless fluxgate magnetometer is varies in the range of 41,660nT to 41,898nT, the H-component magnitude is rapidly increase after sunrise and reach at 42,057nT during noon. The LNO H-component reading is varies in the range of 41,500nT to 41,508nT, increasing rapidly after sunrise until reached at 41,629nT during noon.

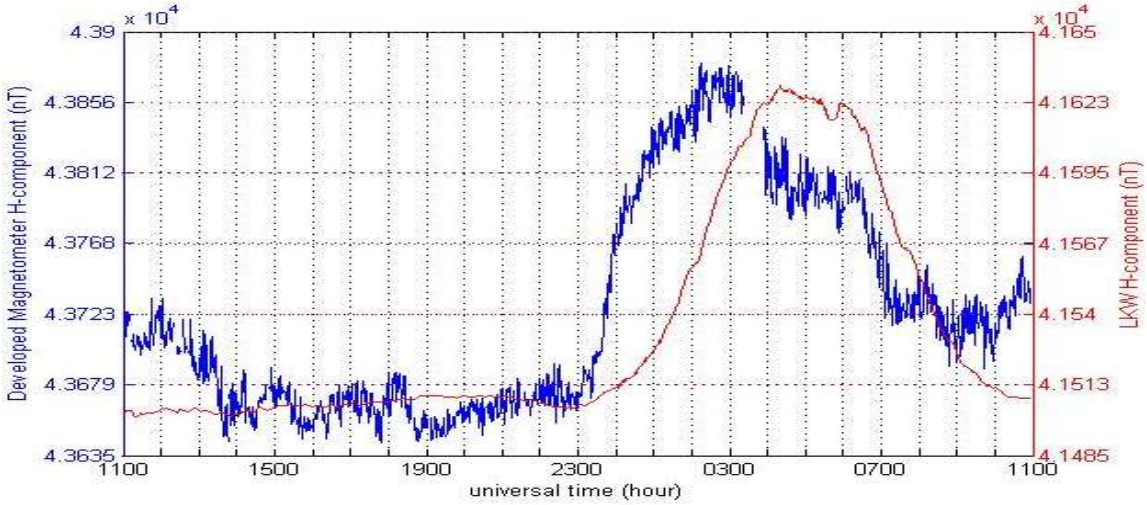

Fig.12. H-component or magnetic north component versus universal time from developed

wireless fluxgate magnetometer (above) and established LNO (below)

The H- and F-component has repetitive and regular pattern of daily variation with a fundamental period of 24-hours. These variation patterns are known as solar quiet variation or SQ variation [13]. The energy and particle transferred from the Sun towards the Earth's sunlit surface is the most intense during midday and charge molecules in the ionosphere produced by ionising radiation (ultraviolet rays and X-ray), which mostly generated at that particular time causing the air conductivity at its highest. After sunset, in the absence of ionising radiation from the Sun, neutral molecules begin to form as the product of ionic charge molecules recombination process since there are absence of ionising radiation. This process occur repetitively every day.

The solar radiation [16] heating the Earth surface causing winds generated. The ionospheric dynamo is drove by thermo-tidal winds, which is combination of winds and tidal winds. The dynamo moving the conductive ionospheric molecules to generate currents. The two closed loops vortexes formed caused by the current generated; an anti-clockwise vortex in the northern hemisphere and a clockwise vortex in the southern hemisphere. These currents influence the daily magnetic field variation as the Earth [14] also rotate creating the day and night variation at one fix reference point. The intensity of solar radiation upon the Earth [15] varies with the solar cycle and seasons changes, which causing Sq variation also manipulated.

For Z-component, the magnitude reading varies in the range of 12,531nT to 12,995nT as can be observed in Fig. 13. The data output of Z-component is consistent with the magnitude range stated in isodynamic chart in Fig. 4 at measurement location point. The isodynamic chart shows the magnitude range at measurement location point is ranging from -10,000nT to -20,000nT.

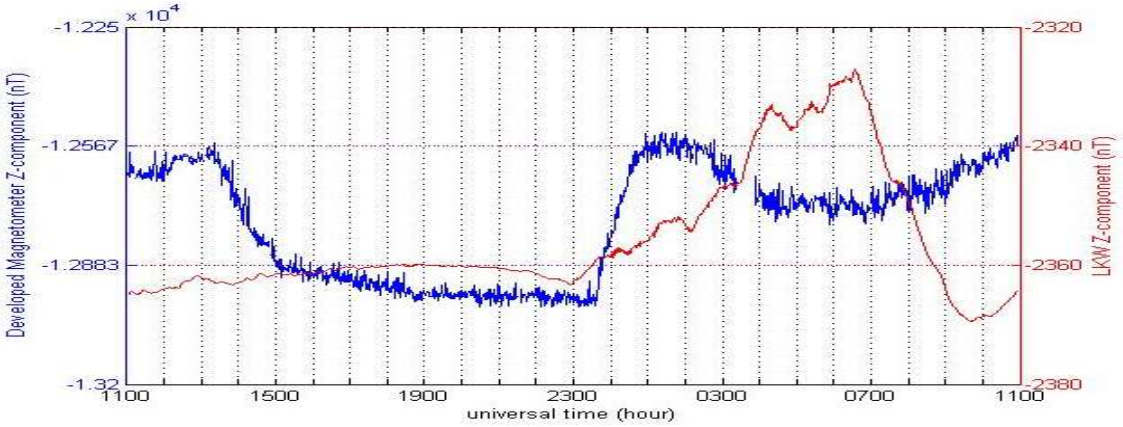

Fig.13. Z-component or vertical downward component versus universal time comparison between wireless fluxgate magnetometer (blue plot) and red plot (LNO)

The F-component magnitude is plotted and compared with LNO F-component on the same graph figure shown in Fig. 14. The data variation from developed wireless fluxgate magnetometer shows consistent data plot pattern with F-component geomagnetic variation from LKW station.

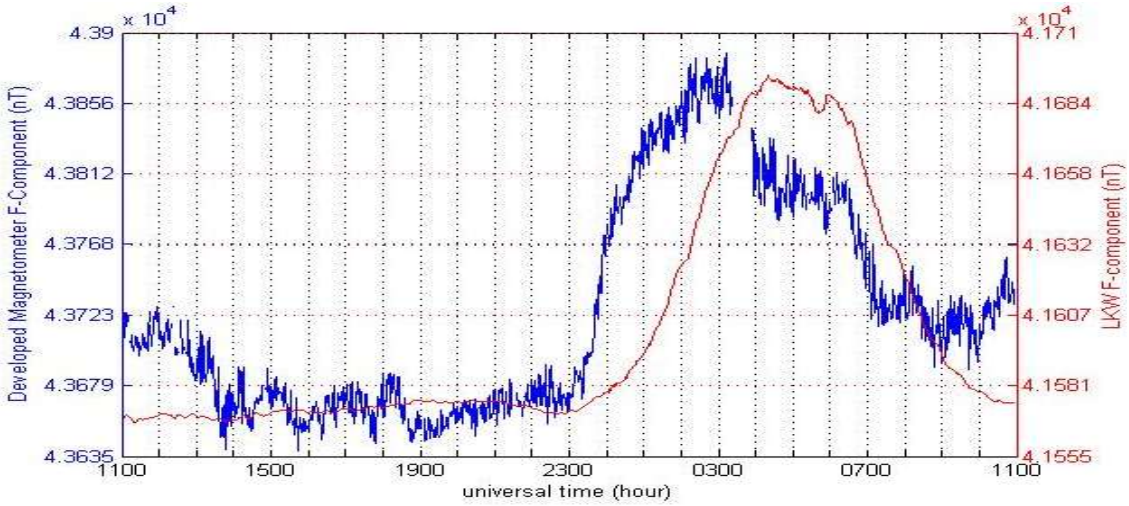

Fig.14. F-component versus universal time from developed wireless fluxgate (blue plot) and LNO (red plot)

The magnitude is varies in the range of 43,631nT to 43,747nT during the absent of sunlight. Right after sunrise, the magnitude is rapidly increasing until reach at 43,893nT during noon. The LNO magnitude is varies in the range of 41,567nT to 41,575nT during the absent of sunlight and rapidly increasing up to 41,695nT during noon.

4. CONCLUSION

The results obtained from the pre-measurement experiment shows that the data output of the developed low power wireless magnetometer approaching accuracy and consistency with existing magnetometer. The device need more pre-measurement experiment and enhanced with advanced signal data processing to obtain smoother data output. The data comparing is the best when the measurement done at the same location point and at the same measurement time. Due to data offline at nearest station point, the data comparing at the same measurement time could not be performed and as an alternative, the most recent geomagnetic variation is compared to the output of the developed magnetometer data output. For the future plan, the magnetometer will be enhanced with advanced signal data processing.

5. ACKNOWLEDGEMENTS

We would like to thank Mr. ShamryMubdiSubraMullisi and his team from Luimewah (M) Sdn. Bhd. for series of helpful discussions and technical support. We would like also to thank UniversitiTeknologi MARA (UiTM) for providing research facilities and platform. We acknowledge British Geological Survey (BGS) for providing the data of world magnetic modelling isodynamic chart. We also acknowledge International Center for Space Weather Science and Education Kyushu University (ICSWSE) and National Space Agency (ANGKASA) for providing magnetic field data reading from their established Magnetic Data Acquisition System (MAGDAS) magnetometer observatory. This work is financially supported by Sultan Mizan Antarctic Research Foundation, YPASM (Code No. YPASM/RGrant/12-2014/JLD.1(23)) and Research Acculturation Grant Scheme, RAGS, (600-RMI/RAGS 5/3 (155/2014)) by Ministry of Education. The authors also would like to thank UniversitiTeknologi MARA for the management support and consideration throughout for project.

6. REFERENCES

[1] Matsuoka A, Shinohara M, Tanaka Y M, Fujimoto A, Iguchi A. Development of fluxgate magnetometers and applications to the space science missions. In K. Oyama, & C. Z. Cheng

(Eds.), An Introduction to Space Instrumentation.Tokyo: Terra Scientific Publishing Company, 2013, pp. 217-225

[2] Dang H B, Malool A C, Romalis M V. Ultra-high sensitivity magnetic field and magnetization measurements with an atomic magnetometer. Applied Physics Letters, 2010, 97(15):1-4

[3] Menk F, Kale Z, Sciffer M, Robinson P, Waters C, Grew R, Cliverd M, Mann I. Remote sensing the plasmasphere, plasmapause, plumes and other features using ground-based magnetometers. Journal Space Weather Climate, 2014, 4(A34):1-16

[4] Owens M J, Horbury T S, Wicks R T, McGregor S L, Savani N P, Xiong M. Ensemble downscaling in coupled solar wind-magnetosphere modelling for space weather forecasting. Space Weather, 2014, 12(6):395-405

[5] Waheed O T, Atiq U R. Design and development of a fluxgate magnetometer for small satellites in low earth orbit. Journal of Space Technology, 2011, 1(1):78-82

[6] Aslam O P M. Study of the solar wind-magnetosphere coupling on different time scales. Planetary and Space Science, 2013,85:123-141

[7] Araki T, Shinbori A. Relationship between solar wind dynamic pressure and amplitude of geomagnetic sudden commencement (SC). Earth, Planets and Space, 2016, 68(1):1-7

[8] Home R B, Glauert S A, Meredith N P, Boscher D, Maget V, Heynderickx D, Pitchford D. Space weather impacts on satellites and forecasting the earth's electron radiation belts with SPACECAST. Space Weather, 2013, 11(4):169-186

[9] van de Kamp M, Seppälä A, Clilverd M A, Rodger C J, Verronen P T, Whittaker I C. A model providing long-term data sets of energetic electron precipitation during geomagnetic storms. Journal of Geophysical Research Atmospheres, 2016, 121(20):12520-12540

[10] Schofield I, Connors M, Russell C T. NetPICOmag: A low-cost networked magnetometer and its applications. Earth, Planets and Space, 2012, 64(3):279-297

[11] Kennedy J, Leveneur J, Turner J, Futter J, Williams G V M. Applications of nanoparticle-based fluxgate magnetometers for positioning and location. In IEEE Sensors Applications Symposium, 2014, pp. 228-232

[12] Ciudad D, Michelena M D, Pérez L, Aroca C. Small fluxgate magnetometers: Development and future trends in Spain. Sensors, 2010, 10(3):1859-1870

[13] Shinbori A, Koyama Y, Nose M. Long-term variation in the upper atmosphere as seen in the geomagnetic solar quiet daily variation. Earth, Planets and Space,2014,66(1):1-20

[14]Farah A M K, Khairunnisa N J, Norbi A A R, Muhammad S J, Mohamad H J, Zairi I R.Implementation of earth conductivity experiment to evaluate underground parameters. ARPN Journal of Engineering and Applied Sciences, 2017, 12(10):3271-3277

[15]Nur A Z, Mohamad H J, Siti Z A Z, Zairi I R. Development of space weather monitoring platform for space and earth's electromagnetism observation. ARPN Journal of Engineering and Applied Sciences, 2017, 12(10):3308-3311

[16]Afifah T, Nor A Z, Atiqah A R, Mohamad H J, Zairi I R.Variation of VHF/UHF of forward scattering radar due to solar radiation. ARPN Journal of Engineering and Applied Sciences, 2017, 12(10):3278-3284

[17]Rina A, Zairi I R, Nik N S N D, Syila I I, Rosmawati S, Mohamad H J. Design an automatic temperature control system for smart tudung saji using Arduino microcontroller.ARPN Journal of Engineering and Applied Sciences, 2016, 11(16):9578-9581

[18]Fadhli D M F, Tatang M, Zairi I R, Mohamad T M, Wan A K W C, Mohamad H J. Supervisory fertigation system using interactive graphical supervisory control and data acquisition system. International Journal on Advanced Science, Engineering and Information Technology, 2016, 6(4):489-494

How to cite this article:
Abidin A F Z, Jusoh M H, Junid S A M A, Razak A H A. Development of low power wireless fluxgate magnetometer instrumentation for real-time geomagnetic monitoring. J. Fundam. Appl. Sci., 2017, *9(5S), 481-497.*